

## Nanoscale Disassembly and Free Radical Reorganization of Polydopamine in Ionic Liquids

Paola Manini, Piero Margari, Christian Silvio Pomelli, Paola Franchi, Gennaro Gentile,  
Alessandra Napolitano, Luca Valgimigli, Cinzia Chiappe, Vincent Ball, and Marco d'Ischia

*J. Phys. Chem. B*, **Just Accepted Manuscript** • DOI: 10.1021/acs.jpcc.6b08835 • Publication Date (Web): 04 Nov 2016

Downloaded from <http://pubs.acs.org> on November 4, 2016

### Just Accepted

“Just Accepted” manuscripts have been peer-reviewed and accepted for publication. They are posted online prior to technical editing, formatting for publication and author proofing. The American Chemical Society provides “Just Accepted” as a free service to the research community to expedite the dissemination of scientific material as soon as possible after acceptance. “Just Accepted” manuscripts appear in full in PDF format accompanied by an HTML abstract. “Just Accepted” manuscripts have been fully peer reviewed, but should not be considered the official version of record. They are accessible to all readers and citable by the Digital Object Identifier (DOI®). “Just Accepted” is an optional service offered to authors. Therefore, the “Just Accepted” Web site may not include all articles that will be published in the journal. After a manuscript is technically edited and formatted, it will be removed from the “Just Accepted” Web site and published as an ASAP article. Note that technical editing may introduce minor changes to the manuscript text and/or graphics which could affect content, and all legal disclaimers and ethical guidelines that apply to the journal pertain. ACS cannot be held responsible for errors or consequences arising from the use of information contained in these “Just Accepted” manuscripts.



**Nanoscale Disassembly and Free Radical Reorganization of Polydopamine in Ionic Liquids**

Paola Manini,<sup>†</sup> Piero Margari,<sup>§</sup> Christian Pomelli,<sup>§</sup> Paola Franchi,<sup>‡</sup> Gennaro Gentile,<sup>¥</sup> Alessandra Napolitano,<sup>†</sup> Luca Valgimigli,<sup>‡\*</sup> Cinzia Chiappe,<sup>§</sup> Vincent Ball,<sup>‡<sup>l</sup></sup> Marco d'Ischia<sup>†\*</sup>

<sup>†</sup>Department of Chemical Sciences, University of Naples Federico II, via Cintia 4, I-80126 Napoli, Italy

<sup>§</sup>Department of Pharmacy, University of Pisa, via Bonanno Pisano 6, I-56126, Pisa, Italy

<sup>‡</sup>Department of Chemistry "G. Ciamician", University of Bologna, via S. Giacomo 2, I-40126 Bologna, Italy

<sup>¥</sup>Istituto per i polimeri compositi e biomateriali, Consiglio Nazionale delle Ricerche, via Campi Flegrei 34, I-80078 Pozzuoli, Italy

<sup>‡</sup>Institut National de la Santé et de la Recherche Médicale, 11 rue Humann, 67085 Strasbourg Cedex, France

<sup>l</sup>Université de Strasbourg, Faculté de Chirurgie Dentaire, 1 Place de l'Hôpital, 67000 Strasbourg, France

**Corresponding Author**

\*Prof. Marco d'Ischia

Phone: +39081674132

Fax: +39081674393

e-mail: [dischia@unina.it](mailto:dischia@unina.it)

\*Prof. Luca Valgimigli

Phone: +390512095683

Fax: +390512095688

e-mail: [luca.valgimigli@unibo.it](mailto:luca.valgimigli@unibo.it)

**ABSTRACT**

Despite the growing scientific and technological relevance of polydopamine (PDA), a eumelanin-like adhesive material widely used for surface functionalization and coating, knowledge of its structural and physicochemical properties, including in particular the origin of paramagnetic behavior, is still far from being complete. Herein, we disclose the unique ability of ionic liquids (ILs) to disassemble PDA, either as suspension or as thin film, up to the nanoscale, and to establish specific interactions with the free radical centers exposed by deaggregation of potential investigative value. Immersion of PDA-coated glasses into four different ILs ( $[\text{C}_1\text{C}_1\text{im}][(\text{CH}_3\text{O})\text{HPO}_2]$ ,  $[\text{C}_1\text{C}_1\text{im}][(\text{CH}_3\text{O})\text{CH}_3\text{PO}_2]$ ,  $[\text{C}_1\text{C}_1\text{im}][(\text{CH}_3\text{O})_2\text{PO}_2]$ ,  $[\text{N}_{1888}][\text{C}_{18:1}]$ ) at room temperature caused the fast and virtually complete removal of the coating as determined by UV-visible spectroscopy and scanning electron microscopy (SEM). Transmission electron microscopy (TEM) analysis of the colored supernatants from PDA suspensions in ILs revealed the presence of nanostructures not exceeding 50 nm in diameter. Electron paramagnetic resonance (EPR) analysis indicated profound IL-dependent modifications in signal intensity, line-width and  $g$ -factor values of PDA. These differences were interpreted in terms of a partial conversion of  $C$ -centered radicals into  $O$ -centered semiquinone-type components following destacking and interaction with the anion component in ILs. The discovery of ILs as a powerful tool to disassemble PDA under mild conditions provides a new entry both to detailed investigations of this biopolymer on the nanoscale and to mild removal of coatings from functionalized surfaces, greatly expanding the scope of PDA-based surface functionalization strategies.

## INTRODUCTION

Deposition of adhesive thin films of polydopamine (PDA), a eumelanin-like insoluble biopolymer produced by autoxidation of dopamine at pH 8.5, has emerged over the past decade as a highly versatile coating methodology for several biomedical and technological applications,<sup>1-3</sup> including surface modification of inorganic materials,<sup>4,5</sup> molecular sieve membranes,<sup>6</sup> polymer grafting,<sup>7</sup> multifunctional nanoparticles,<sup>8,9</sup> cell and droplet coating,<sup>10</sup> electronic devices, biointerfaces,<sup>11</sup> biosensors<sup>12-14</sup> and drug delivery.<sup>15,16</sup> PDA appears to consist of a heterogeneous mixture of oligomeric components made up of uncyclized dopamine units, cyclized 5,6-dihydroxyindole (DHI) units and degraded pyrrolecarboxylic acid moieties.<sup>17-19</sup> The importance of aggregation phenomena and physical interactions in PDA buildup and overall morphology has also been emphasized. Studies of PDA film growth have yielded considerable insights into the mechanisms of the process highlighting the important influence of oxidation conditions on the spectral and physical-chemical characteristics of films, coatings and particles. Depending on whether dopamine autoxidation is carried out in Tris, bicarbonate or phosphate buffer, PDA films with different chemical composition and properties can be obtained, reflecting in part the incorporation of Tris into the growing PDA scaffolds.<sup>20</sup> Even more remarkable is the role of the oxidant and pH of the medium, as indicated by the production of superhydrophilic/superoleophobic PDA thin films by oxidation of dopamine with excess periodate in an acidic medium.<sup>21</sup> Strategies for modifying PDA properties via structural modification or copolymerization with suitable substrates have also been reported.<sup>22,23</sup> Along with studies on structure and properties, increasing attention is currently being directed to elucidate the nature and origin of PDA paramagnetic properties. This is a topic of both scientific and practical relevance, since there is evidence that the EPR behavior of eumelanin polymers reflects the  $\pi$ -electron properties of the materials that underlie their both light absorption, antioxidant, redox activity and conductivity properties. In particular, EPR spectroscopy may be a most useful approach to disentangle the effects of intermolecular and intramolecular contributions to the electronic properties of complex disordered insoluble systems by comparing spectral parameters on solid state

1  
2  
3 and de-aggregated samples.<sup>24</sup> The majority of available information on PDA free radicals comes  
4  
5 from two recent reports. In the first,<sup>20</sup> the EPR spectra of three different samples prepared in Tris,  
6  
7 phosphate and bicarbonate buffer were compared to gain an insight into the effects of buffer-  
8  
9 dependent structural modifications and aggregation mechanisms on the paramagnetic centers as  
10  
11 probes of the  $\pi$ -electron system. Similar single, roughly symmetric signals were determined for all  
12  
13 samples at a  $g$  value of  $\sim 2.004$ , typical of carbon-centered radicals. A significantly broader signal  
14  
15 was however observed in the sample prepared from Tris buffer, reflecting apparently the  
16  
17 superposition of two main signals and interpreted as being due to the simultaneous presence of  
18  
19 carbon-centered radicals and semiquinone radicals.<sup>25</sup> Moreover, normalized power saturation  
20  
21 profiles indicated for the PDA-Tris sample a lower degree of molecular disorder and intermolecular  
22  
23 spin delocalization, due probably to a lower tendency to aggregation and stacking caused by  
24  
25 incorporation of Tris, hindering delocalization of the paramagnetic centers across the molecular  
26  
27 scaffolds.

28  
29  
30  
31 In another report,<sup>26</sup> the EPR properties of PDA samples were investigated in detail. For all samples  
32  
33 a single unresolved signal was observed with a slightly asymmetrical line in a broad range of  
34  
35 temperature.  $g$ -Factor measurements gave a relatively constant value as  $\sim 2.0052$  in a PDA-Tris  
36  
37 sample (17% wt of H<sub>2</sub>O) in a broad temperature range, and  $\sim 2.0038$  in a PDA-phosphate sample  
38  
39 (8.2% wt of H<sub>2</sub>O), slightly decreasing below 100 K. It was concluded that both the moisture content  
40  
41 and the type of buffer used during PDA synthesis have an influence on the spectral parameters. A  
42  
43 marked line broadening was apparent moreover at liquid helium temperatures, supposedly due to  
44  
45 enhancement of the relaxation rate.

46  
47  
48  
49 Related studies carried out on synthetic eumelanins,<sup>25</sup> showed that the water content has a strong  
50  
51 influence on the solid-state EPR signal of eumelanins, causing a decrease in spin density as it  
52  
53 increases. On the other hand, the  $g$  values in the solid state are not greatly affected by changes in pH  
54  
55 or hydration level. Based on these results, it was concluded that: 1) the solid-state EPR signal of  
56  
57 eumelanin may not arise from a dominant semiquinone free radical ( $g \approx 2.0045$  to  $2.005$ ) but rather  
58  
59

1  
2  
3 from a dominant carbon-centered free radical ( $g \sim 2.0036$ ); 2)  $\pi$ - $\pi$  destacking, brought about by the  
4  
5 addition of water or increased pH may increase the proportion of semiquinone radicals via a  
6  
7 comproportionation reaction, leading to the exposure and partial abatement of the carbon-centered  
8  
9 spin in the wet environment. Although these data provided direct or indirect insights into PDA  
10  
11 paramagnetic properties, supporting potential utilization for imaging applications, the actual nature  
12  
13 of the species responsible for the paramagnetic behavior of PDA and the role of  
14  
15 aggregation/stacking remain poorly understood.

16  
17  
18 On the basis of previous observations pointing to inhibition of aggregation as a useful means of  
19  
20 probing eumelanin paramagnetic properties,<sup>24</sup> we set up a series of experiments aimed at exploring  
21  
22 for the first time the variations in the paramagnetic properties of PDA following  
23  
24 deaggregation/destacking under mild non-destructive conditions. This looked at the onset as a most  
25  
26 challenging goal considering the notorious resistance of eumelanin-type materials to dissolution or  
27  
28 deaggregation without making recourse to harsh treatments with alkali and heating. Although it was  
29  
30 reported that treatment with aqueous ammonia can induce eumelanin destacking,<sup>27</sup> the occurrence  
31  
32 and consequences of alkali-induced oxidative breakdown processes modifying the polymer  
33  
34 backbone and spin properties via *o*-quinone cleavage were not addressed. In searching for  
35  
36 alternative non-basic systems capable of inducing non-destructive deaggregation of PDA we turned  
37  
38 out attention to ionic liquids (ILs) as a promising tool to probe paramagnetic properties via  
39  
40 destacking and physical interaction with the paramagnetic centers. Use of ILs for studies of PDA  
41  
42 was suggested by the following considerations: a) ILs are a unique class of solvents so far little  
43  
44 explored in EPR spectroscopy, which display high polarity, extraordinarily high viscosity, and can  
45  
46 form nano-mesoscale polar and nonpolar domains that appear to be optimally suited to probe the  
47  
48 effects of specific ionic interactions and diffusion/mobility-controlled processes on free radical  
49  
50 properties of heterogeneous systems like eumelanins,<sup>28,29</sup> b) ILs can promote metal-free  
51  
52 depolymerization of phenolic polymers, thus suggesting a potential use to disentangle compact  
53  
54  
55  
56  
57  
58  
59  
60

1  
2  
3 PDA components;<sup>30</sup> c) ILs have surface tensions suitable to induce direct exfoliation of graphite and  
4  
5 stabilization of exfoliated graphene via Coulombic interaction.

6  
7 Aim of this study was to assess the ability of ILs to induce deaggregation of PDA and to probe the  
8  
9 changes occurring in PDA free radical properties upon destacking and interactions with this  
10  
11 peculiar ionic medium.  
12

## 13 14 15 16 **EXPERIMENTAL SECTION**

17  
18 **Synthesis of dimethylimidazolium dimethylphosphate ([C<sub>1</sub>C<sub>1</sub>im][(CH<sub>3</sub>O)<sub>2</sub>PO<sub>2</sub>]),**  
19  
20 **dimethylimidazolium methyl-methylphosphonate ([C<sub>1</sub>C<sub>1</sub>im][(CH<sub>3</sub>O)CH<sub>3</sub>PO<sub>2</sub>]), and**  
21  
22 **dimethylimidazolium methylphosphonate ([C<sub>1</sub>C<sub>1</sub>im][(CH<sub>3</sub>O)HPO<sub>2</sub>]).** 1-Methylimidazole (1 eq)  
23  
24 and the alkylating agent (trimethyl phosphate or dimethyl-methyl phosphonate or dimethyl  
25  
26 phosphite, 1.1 eq), mixed at room temperature under argon and vigorous stirring, were heated at  
27  
28 110 °C for 24 h. Then the mixture was repeatedly washed with anhydrous diethyl ether to remove  
29  
30 the excess of reagent and the recovered liquid was dried under *vacuum* for 24-48 h at 80 °C.  
31

32  
33 Structure and purity of the recovered transparent liquids (yields 95-97%) were checked by NMR  
34  
35 analysis. *N*-methyl-*N,N*-dioctylammonium oleate ([N<sub>1888</sub>][C<sub>18:1</sub>]) was synthesized by a two-step  
36  
37 procedure using the same experimental conditions described in literature.<sup>31</sup>  
38

39  
40 **SEM and TEM analysis.** SEM analysis was performed by means of a FEI-Quanta 200-FEG using  
41  
42 secondary electron detector and an acceleration voltage of 10-30 kV. Before the analysis the sample  
43  
44 was sputter coated with a 10 nm-thick Au/Pd layer. TEM analysis was performed in bright field  
45  
46 mode using a FEI-Tecna G12 Spirit Twin (LaB6 source) operating at 120 kV. Carbon coated TEM  
47  
48 grids were immersed in the PDA suspensions. Before the analysis, in order to better evidence the  
49  
50 PDA nanostructures, except for the sample obtained from [C<sub>1</sub>C<sub>1</sub>im][(CH<sub>3</sub>O)CH<sub>3</sub>PO<sub>2</sub>] suspension, it  
51  
52 was necessary to remove ILs by washing the grids with distilled water (sample from  
53  
54 [C<sub>1</sub>C<sub>1</sub>im][(CH<sub>3</sub>O)CH<sub>3</sub>PO<sub>2</sub>]) or ethyl acetate (samples from [C<sub>1</sub>C<sub>1</sub>im][(CH<sub>3</sub>O)HPO<sub>2</sub>] and  
55  
56 [N<sub>8881</sub>][C<sub>18:1</sub>]).  
57  
58  
59  
60

**EPR spectroscopy.** X-Band EPR spectra were recorded at 298K on a Bruker Elexsys E500 spectrometer equipped with an ER 049 Super X MW bridge and VT 1000 variable temperature unit. Spectra consisted of two accumulated scans set at MW power = 2.5 mW, modulation amplitude = 1.0 G, modulation frequency = 100 kHz. Samples were placed in a 200  $\mu$ L calibrated glass tube sitting inside a 4 mm id quartz tube, accurately positioned inside the cavity. For sample in ILs 35  $\mu$ L of solution were analyzed, so to cover the entire sensitive area in the cavity. For solid state samples 0.2 to 2.5 mg were analyzed. Measured *g*-factors were corrected with respect to that of a standard sample of perylene radical cation in concentrated H<sub>2</sub>SO<sub>4</sub> (*g* = 2.00258) and checked against the measured value for 2,2-diphenyl-1-picrylhydrazyl radical (DPPH•) at the solid state (*g* = 2.0036). For quantitative analysis of solid state samples the double integral of EPR signal was compared to that of different samples of DPPH• powder in the same calibrated tube. For PDA samples in IL, the spectrometer response was calibrated with standard solutions of DPPH• in the same ionic liquids. For higher relative accuracy only the strongest EPR signals corresponding to PDA samples in [N<sub>8881</sub>][C<sub>18:1</sub>] were calibrated using the double integral: spin/L values for samples in the other ILs were determined based on samples in [N<sub>8881</sub>][C<sub>18:1</sub>] by comparing the normalized signal intensity. Signal intensities (*I*) were normalized by the square of line width (*W*) according to eq. 1. As an independent assessment of radical concentration, the normalized signal intensity were normalized against the UV absorbance of the sample at 400 nm, according to eq. 2.

$$I(\text{norm}) = I \cdot W^2 / W_{(\text{ref})}^2 \quad (1)$$

$$I/A_{400}(\text{norm}) = I(\text{norm}) \cdot A_{400(\text{ref})} / A_{400} \quad (2)$$

## RESULTS AND DISCUSSION

**Synthesis of PDA and preparation of PDA thin films.** PDA and PDA thin films on glass have been prepared according to a procedure reported in the literature.<sup>32</sup> Briefly, a solution of dopaminehydrochloride has been dissolved in the appropriate buffer, that is Tris or bicarbonate buffer (0.05 M, pH 8.5), and left under vigorous stirring for 24 h. The PDA powder has been collected after acidification of the reaction mixture and centrifugation at 4 °C. PDA thin films have

been prepared by dipping of a glass substrate in the reaction mixture. After 2 h, the glass substrate has been rinsed thoroughly with pure water and dried under nitrogen flux to afford a quite homogeneous film with a thickness set in the 50-60 nm range.

**Selection of ILs and PDA solubility tests.** Studies of PDA destacking were carried out using in four different ILs, namely 1,3-dimethylimidazolium dimethylphosphate,  $[\text{C}_1\text{C}_1\text{im}][(\text{CH}_3\text{O})_2\text{PO}_2^-]$ , 1,3-dimethylimidazolium methyl-methylphosphate  $[\text{C}_1\text{C}_1\text{im}][(\text{CH}_3\text{O})\text{CH}_3\text{PO}_2^-]$ , 1,3-dimethylimidazolium methylphosphate  $[\text{C}_1\text{C}_1\text{im}][(\text{CH}_3\text{O})\text{HPO}_2^-]$  and *N*-methyl-*N,N*-dioctylammonium oleate,  $[\text{N}_{8881}][\text{C}_{18:1}]$  (Chart 1).

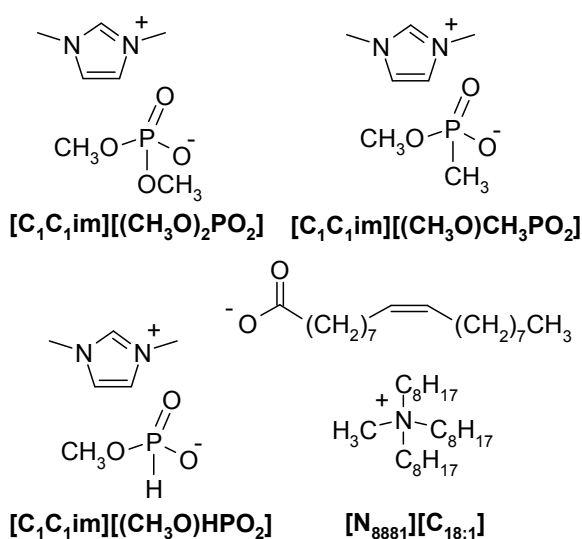
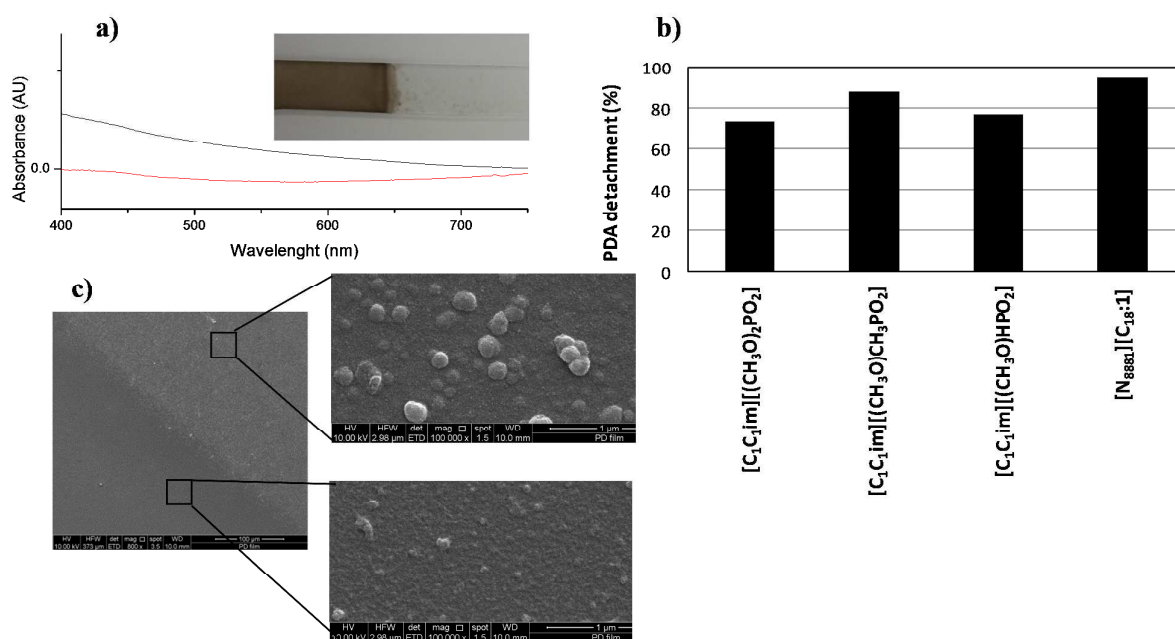


**Chart 1.** Structure of ILs used in this study.

Since the intercalation of ILs into polymeric materials depends on ILs' anions and cations, being determined by the nature of the chemical interactions that these two components are able to establish, we decided to focalize our attention on ILs having strong hydrogen bond acceptor anions.<sup>33</sup> These anions should be indeed able to interact with most of the functional group present on PDA. Halogen free and hydrolytically stable ILs based on dimethylphosphate and phosphonate anions were selected, associating as cation the small dimethylimidazolium. ILs based on imidazolium cations are indeed highly effective for the exfoliation of bundled single-wall nanotubes

and graphene, probably due to the proposed ability to adhere strongly to the  $\pi$ -conjugated graphitic surface, most probably via cation- $\pi$  interactions. It is worth of note that in the presently used ILs the small alkyl substituents present both on cation and anion practically nullify the apolar component characterizing the three-dimensional network of most ILs, generally consisting of polar and apolar domains,<sup>34</sup> making the eventual role of the cation- $\pi$  interactions dominant. However, since it has been shown that some ILs bearing long alkyl chains are able to promote the debundling of carbon nanotubes,<sup>35</sup> we decided to investigate also an ammonium salt bearing three long alkyl chains on cation and a long alkyl unsaturated chain on anion,  $[N_{8881}][C_{18:1}]$ . This IL, having oleate as anion, associates a high hydrogen bond acceptor ability to an apolar nature.

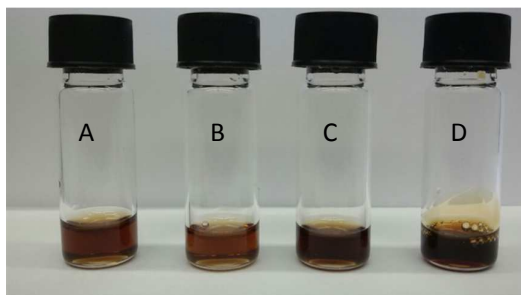
In preliminary experiments, the effects of the ILs on PDA was investigated using thin films on glass. Spectrophotometric analyses showed marked decrease in the absorbance at 400 nm of the coated regions following immersion in ILs for 16 hours with respect to the untreated coated glass as internal reference (Figure 1). Specifically, the following percent absorbance decrease values at 400 nm were determined:  $[C_1C_{1im}][(\text{CH}_3\text{O})_2\text{PO}_2]$ , 74%;  $[C_1C_{1im}][(\text{CH}_3\text{O})\text{CH}_2\text{PO}_2]$ , 88%;  $[C_1C_{1im}][(\text{CH}_3\text{O})\text{HPO}_2]$ , 77%; and  $[N_{8881}][C_{18:1}]$ , 95%.



1  
2  
3 **Figure 1.** Effect of ILs on PDA thin film detachment from glass. a) Visible absorption profiles of  
4 PDA thin film on glass before (black trace) and after (red trace) immersion in  $[\text{N}_{8881}][\text{C}_{18:1}]$ . In the  
5 inset is reported the border between the treated and untreated region of the PDA thin film on glass.  
6  
7  
8  
9  
10 b) Percentage of thin film detachment after treatment with IL expressed as the ratio between the  
11 absorbance at 400 nm of the treated and untreated thin films. c) Secondary electron SEM images of  
12 the border region between the treated and untreated PDA film on glass: at high magnification the  
13 original film morphology (up-right) and the almost complete removal after exposure of the glass  
14 substrate to  $[\text{N}_{8881}][\text{C}_{18:1}]$  (down-right) is well apparent.  
15  
16  
17  
18  
19  
20  
21  
22

23 Scanning electron microscopy (SEM) analysis revealed significant modifications in the IL-exposed  
24 area with respect to the unexposed surface (Figure 1c).  
25  
26

27 In separate experiments, PDA samples produced under two different conditions, i.e. by autoxidation  
28 of dopamine in Tris buffer or in bicarbonate buffer at pH 8.5, were suspended in the previously  
29 desiccated ILs at a concentration of 1 mg/ml and were sonicated for 30 min in an ice bath. The  
30 resulting suspensions were carefully centrifuged to remove a small residue which was not treated  
31 further, and the clear supernatants, exhibiting dark colorations (Figure 2), were examined by UV-  
32 visible spectroscopy.  
33  
34  
35  
36  
37  
38  
39



50  
51 **Figure 2.** Supernatants from PDA-Tris dispersion in ILs: From left to right:

52  $[\text{C}_1\text{C}_1\text{im}][(\text{CH}_3\text{O})\text{HPO}_2]$  (A),  $[\text{C}_1\text{C}_1\text{im}][(\text{CH}_3\text{O})_2\text{PO}_2]$  (B),  $[\text{C}_1\text{C}_1\text{im}][(\text{CH}_3\text{O})\text{CH}_3\text{PO}_2]$  (C),  
53  
54  
55  $[\text{N}_{8881}][\text{C}_{18:1}]$  (D).  
56  
57  
58  
59  
60

1  
2  
3 The results (see Supporting Information) showed in all cases almost featureless curves spanning the  
4 entire UV-visible range. Taking the absorbance at 400 nm as a reference, the relative amount of  
5 PDA in the various ILs could be estimated assuming similar visible extinction coefficients for the  
6  
7  
8  
9  
10 two PDA samples. PDA-Tris proved to be slightly more soluble than PDA bicarbonate in  
11  
12 dimethylimidazolium-based ILs, in line with the smaller aggregate size of PDA-Tris.<sup>20</sup> However,  
13  
14 judging from absorbance values, both PDA samples proved to be slightly more dispersible in  
15  
16 [N<sub>8881</sub>][C<sub>18:1</sub>], the more hydrophobic of the tested ILs.

17  
18 To gain deeper insight into PDA-IL interactions, the supernatants from PDA suspension in ILs were  
19  
20 examined by transmission electron microscopy (TEM). Data in Figure 3 revealed the presence of  
21  
22 scattered PDA nanostructures not exceeding 50 nm in size which on closer inspection proved to  
23  
24 consist in turn of aggregates of much smaller components.  
25  
26  
27  
28  
29  
30  
31  
32  
33  
34  
35  
36  
37  
38  
39  
40  
41  
42  
43  
44  
45  
46  
47  
48  
49  
50  
51  
52  
53  
54  
55  
56  
57  
58  
59  
60

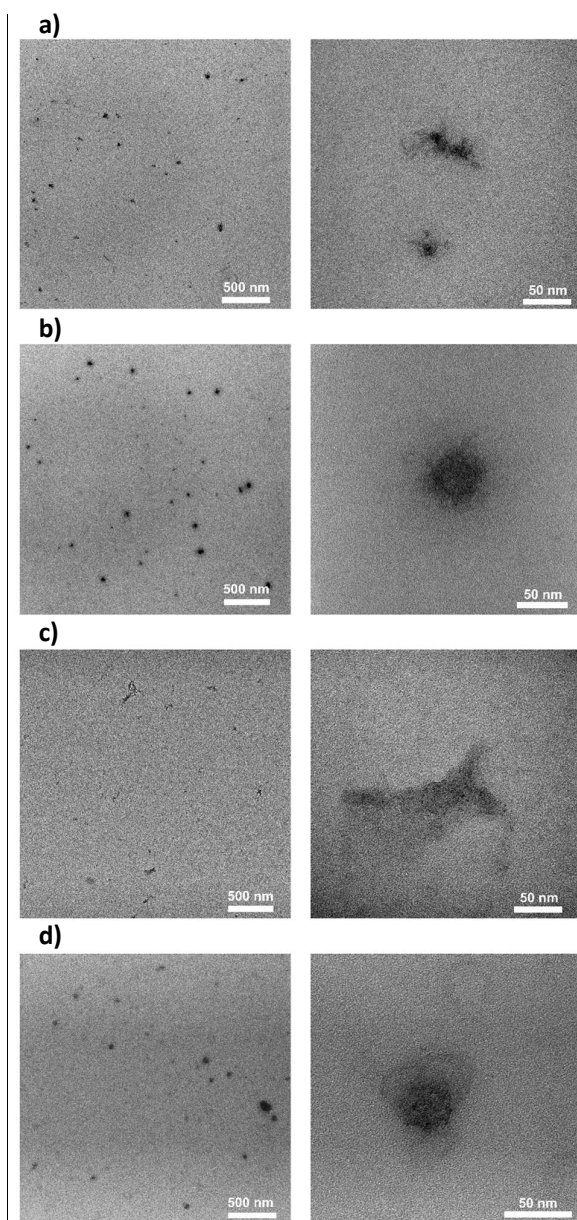


**Figure 3.** Bright field TEM images of nanostructures obtained by sonication of PDA in ILs. a)  $[\text{C}_1\text{C}_1\text{im}][(\text{CH}_3\text{O})\text{HPO}_2]$ , b)  $[\text{C}_1\text{C}_1\text{im}][(\text{CH}_3\text{O})\text{CH}_3\text{PO}_2]$ , c)  $[\text{C}_1\text{C}_1\text{im}][(\text{CH}_3\text{O})_2\text{PO}_2]$ , d)  $[\text{N}_{1888}][\text{C}_{18:1}]$ .

**EPR analysis.** Based on these results, the EPR response of the various PDA-containing ILs was next examined using X-band spectroscopy, which had previously been successfully employed to investigate the paramagnetic properties of melanins in the solid state.<sup>25</sup> Data reported in Table 1

showed a detectable EPR signal in all cases, with varying intensity apparently unrelated to UV-vis absorbance values, suggesting different IL-dependent free radical properties.

**Table 1.** X-band EPR spectral parameters recorded for PDA samples in ionic liquids and in the solid state at 298 K.

<b>Ionic Liquid<sup>a</sup></b>	<b>PDA-Tris</b>	<b>PDA-bicarbonate</b>
$[\text{C}_1\text{C}_1\text{im}][(\text{CH}_3\text{O})_2\text{PO}_2]^\text{b}$	$g = 2.00400$ $W = 5.3 \text{ G}, I = 31680$	$g = 2.00362$ $W = 6.3 \text{ G}, I = 14630$
$[\text{C}_1\text{C}_1\text{im}][(\text{CH}_3\text{O})\text{CH}_3\text{PO}_2]^\text{b}$	$g = 2.00456$ $W = 5.5 \text{ G}, I = 36866$	$g = 2.00359$ $W = 6.8 \text{ G}, I = 16019$
$[\text{C}_1\text{C}_1\text{im}][(\text{CH}_3\text{O})\text{HPO}_2]^\text{b}$	$g = 2.00443$ $W = 5.3 \text{ G}, I = 23659$	$g = 2.00365$ $W = 6.3 \text{ G}, I = 13396$
$[\text{N}_{8881}][\text{C}_{18:1}]^\text{b}$	$g = 2.00473$ $W = 6.9 \text{ G}, I = 107000$	$g = 2.00480$ $W = 6.4 \text{ G}, I = 126000$
None: powder <sup>c</sup>	$g = 2.00346$ $W = 4.8 \text{ G}, I = 3.25 \times 10^5$	$g = 2.00336$ $W = 4.6 \text{ G}, I = 2.47 \times 10^5$

<sup>a</sup> Neat ionic liquids had no detectable EPR signal. <sup>b</sup> Recorded on 35  $\mu\text{L}$  of saturated IL solution. <sup>c</sup> Recorded on 0.5 mg of solid state sample.

As a rule, PDA-Tris displayed more intense signals than PDA-bicarbonate. Significantly stronger signals for both samples were determined however in  $[\text{N}_{8881}][\text{C}_{18:1}]$ , on account of a good solubilization, regardless of the mode of preparation of the PDA sample, i.e. Tris or bicarbonate, while the weakest signals are observed in  $[\text{C}_1\text{C}_1\text{im}][(\text{CH}_3\text{O})\text{HPO}_2]$ . This suggests that solubilization/deaggregation effects depending on solvent polarity play an important role in IL-PDA spin interactions, possibly also influencing different spin populations in the eumelanin-type materials. An increase in signal intensity was previously reported for the complexes of DOPA melanin with gentamycin and kanamycin.<sup>36</sup> Consistent with a different EPR behavior, a comparative view of the main EPR spectral parameters, i.e.  $g$ -value and signal amplitude ( $W$ ), for the two PDA samples showed marked differences depending both on the sample and nature of the IL. Overlays of spectra of the PDA samples in the various ILs, recorded at 298 K under identical settings are given in Figure 4 along with the corresponding spectra recorded on the same PDA samples in the solid state.

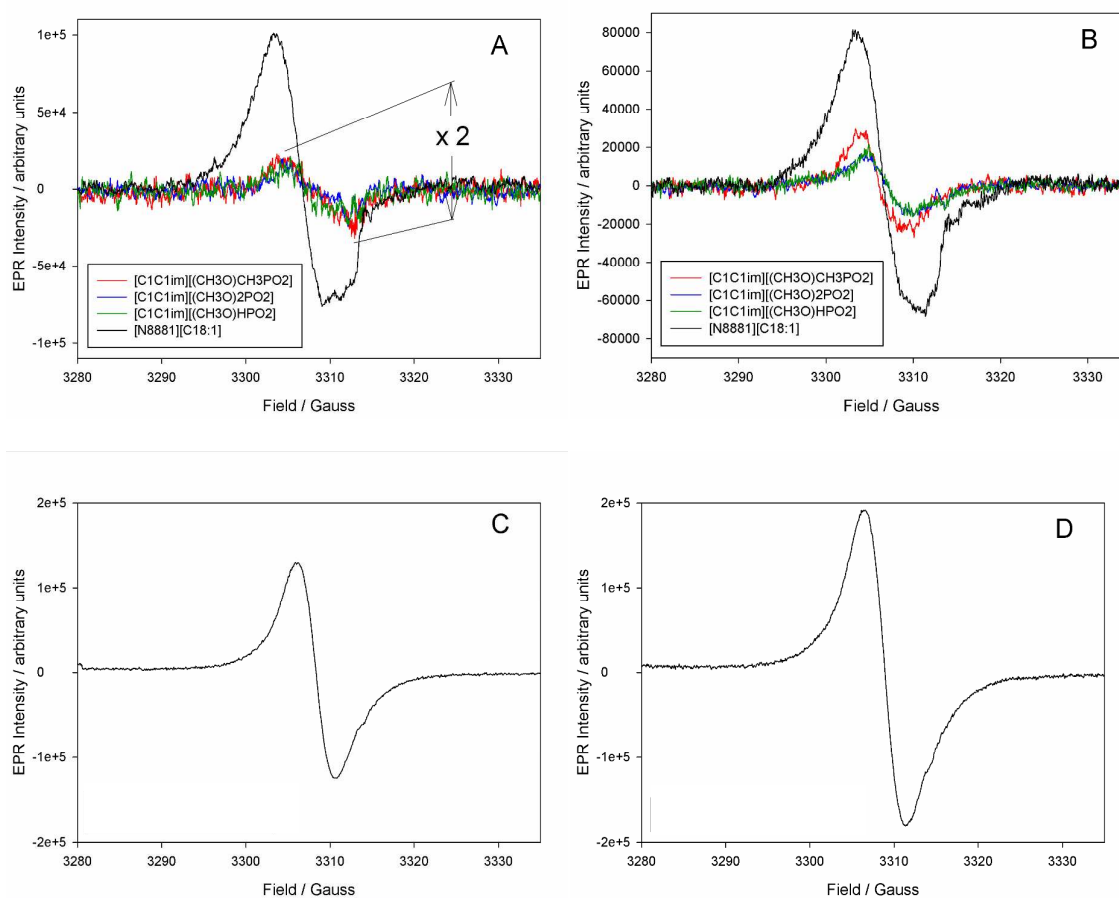


**Figure 4.** EPR spectra of PDA melanin prepared in bicarbonate (A and C) or Tris buffer (B and D) suspended in ILs as indicated (A and B, 35  $\mu\text{L}/\text{sample}$ ) or in the solid state (C and D, 0.5 mg/sample). In A spectra in  $[\text{C}_1\text{C}_1\text{im}][(\text{CH}_3\text{O})_2\text{PO}_2]$ -based ILs have been upscaled by a factor of 2 for easier viewing.

Comparison of  $g$ -factor values in Table 1 showed that the two PDA samples show similar values in the solid state, PDA-Tris being just slightly shifted downfield; however, they exhibit significant differences in ILs. In particular, while PDA-bicarbonate displayed a modest increase of  $g$ -factor in 1,3-dimethylimidazolium-based ILs compared to the solid state (ca. 2.0036 vs. ca. 2.0034), PDA-Tris exhibited markedly downfield shifts in the same three solvents, with  $g$  ranging between 2.0040-2.0046. An even larger shift was noted however for both PDA samples in  $[\text{N}_{8881}][\text{C}_{18:1}]$ . A possible conclusion from these data, based also on previous evidence<sup>20,37</sup> is that ILs can tip the balance of C-

centered and *O*-centered radicals toward the latter, which would be rescued from aggregation dependent quenching effects.<sup>25</sup> Most likely, the ionic nature of the medium and especially the basicity of the anion promotes the generation of charged semiquinone radical species in a similar manner as an increase in pH, i.e. by shifting the quinone/hydroquinone to semiquinone equilibrium,<sup>25</sup> or by promoting quinone-like radical cations and anions.<sup>38</sup> Comparing the relative basicity of the anions in the various ionic liquids ( $pK_a$   $[(CH_3O)_2PO_2]H = 1.29$ ,  $[(CH_3O)CH_2PO_2]H = 2.31$ ,  $[(CH_3O)HPO_2]H = 2.05$ ,  $[C_{18:1}]H = 4.78$ ) it can be argued that the marked shift in the resonant field in  $[N_{8881}][C_{18:1}]$  is due to the stronger basicity of the carboxylate anion compared to phosphate/phosphonate anions. On the other hand, the peculiar structural features of this IL, characterized by large apolar hydrocarbon domains interconnected in a bicontinuous, sponge-like nanostructure, could also affect this parameter. The higher *g* values of PDA-Tris relative to PDA-bicarbonate in the solid state as well as in all tested ILs may reflect the effect of the Tris moieties incorporated into the PDA scaffolds, which would favor the generation of semiquinone-type free radical species as previously observed in the solid state.<sup>20</sup>

Data in Table 1 revealed for PDA/bicarbonate and, to a lesser extent PDA-Tris, a marked broadening of the EPR signal (*W*) when recorded in ILs with respect to the solid state. In principle, signal broadening in the ILs compared to the solid state might reflect a higher degree of spin delocalization in the eumelanin components as freed from the constraints of the solid state. When viewed in the light of the *g*-factor values, *W* data in 1,3-dimethylimidazolium based ILs, but not  $[N_{8881}][C_{18:1}]$ , revealed an opposite behavior for the two PDA samples: significant *g*-value shifts were related to more modest broadening, while more modest *g* factor shift was associated to the larger broadening.

**Table 2.** EPR signal intensity normalized on line width and on UV-Vis absorbance and corresponding quantitative radical concentration for PDA melanins suspended in ionic liquids

Melanin / IL	$I/W(\text{norm})^a$	$I/A_{400}(\text{norm})^b$	$N \times \text{spins}/L^c$
--------------	----------------------	----------------------------	-----------------------------

<b>PDA-Tris</b>			
[C <sub>1</sub> C <sub>1</sub> im][(CH <sub>3</sub> O) <sub>2</sub> PO <sub>2</sub> ]	29525	19683	5.91×10 <sup>-5</sup>
[C <sub>1</sub> C <sub>1</sub> im][(CH <sub>3</sub> O)CH <sub>3</sub> PO <sub>2</sub> ]	37000	37000	6.30×10 <sup>-5</sup>
[C <sub>1</sub> C <sub>1</sub> im][(CH <sub>3</sub> O)HPO <sub>2</sub> ]	22050	10500	5.53×10 <sup>-5</sup>
[N <sub>8881</sub> ][C <sub>18:1</sub> ]	169020	56339	1.31×10 <sup>-4</sup>
<b>PDA-bicarbonate</b>			
[C <sub>1</sub> C <sub>1</sub> im][(CH <sub>3</sub> O) <sub>2</sub> PO <sub>2</sub> ]	19266	19266	5.38×10 <sup>-5</sup>
[C <sub>1</sub> C <sub>1</sub> im][(CH <sub>3</sub> O)CH <sub>3</sub> PO <sub>2</sub> ]	24576	24576	5.66×10 <sup>-5</sup>
[C <sub>1</sub> C <sub>1</sub> im][(CH <sub>3</sub> O)HPO <sub>2</sub> ]	17641	10377	5.30×10 <sup>-5</sup>
[N <sub>8881</sub> ][C <sub>18:1</sub> ]	171232	68493	1.33×10 <sup>-4</sup>

<sup>a</sup>  $I/W(\text{norm}) = \text{EPR signal intensity normalized on EPR line width } (I \cdot W^2 / W^2_{(\text{ref})})$ . <sup>b</sup>  $I/A_{400}(\text{norm}) = \text{EPR signal intensity normalized both on EPR line width and on UV absorbance at 400nm}$ . <sup>c</sup>  $N \times \text{spins/L} = \text{concentration of radicals (unpaired electrons) in the IL suspension (corresponding to molar concentration in solution)}$ .

Since linewidth (W) in EPR spectra of melanin samples varied significantly and intensity (I) is known to be reversely proportional to the square of the linewidth, in order to compare EPR signal intensities for the different samples, all spectra were normalized against  $W^2$ . Absolute values of radical concentration in suspension were also estimated upon calibration of the spectrometer response, by comparison of the double integral of the signal intensity with that recorded for standard solutions of persistent 2,2-diphenyl-1-picrylhydrazyl radical (DPPH•) in the same ionic liquid. The result expressed as Avogadro's  $N \times \text{spins} / \text{L}$  would provide the apparent molar concentration of radicals (or unpaired electrons) in the different ionic liquids (Table 2). Of interest, this quantity clusters around  $3.5 \times 10^{19}$  spins / L in the three 1,3-dimethylimidazolium-based ILs, and is more than twice as large in [N<sub>8881</sub>][C<sub>18:1</sub>], irrespective of the mode of synthesis (Tris or bicarbonate) of the PDA sample. For comparison, the number of spins per mg of sample was also estimated for solid state PDA samples upon calibration of the spectrometer response with solid state DPPH• radical. The results indicate that our PDA-Tris and PDA-bicarbonate samples had respectively  $3.5 \times 10^{15}$  and  $2.2 \times 10^{15}$  spins/mg, which are in excellent agreement with the values in the range  $2.4 \times 10^{15}$  to  $3.8 \times 10^{15}$  spins/mg recently reported for solid state PDA-Tris, respectively by L-band and X-band EPR spectroscopy.<sup>26</sup>

As an independent assessment of the relative concentration of suspended radicals, the normalized EPR signal intensities were normalized again against the visible absorbance values of the IL solutions, that is, the EPR signal intensity/ $A_{400}$  ratio was taken as an arbitrary index of unpaired electron concentration in ILs. Again it was found that the highest radical concentration can be detected in  $[N_{8881}][C_{18:1}]$  regardless of the mode of preparation of the PDA sample, i.e. Tris or bicarbonate, while the lowest is observed in  $[C_1C_{1im}][[(CH_3O)HPO_2]]$ . This calibration, however, offered interesting insights concerning the role of ILs in affecting the paramagnetic properties of PDA. A plot of EPR normalized signal intensity versus  $I/A_{400}$  normalized signal shows a roughly linear dependence in 1,3-dimethylimidazolium-based ILs, with values in  $[N_{8881}][C_{18:1}]$  clearly escaping such correlation (Figure 5). This suggests that the ionic liquid affects the EPR signal in different ways. Namely, 1,3-dimethylimidazolium-based ILs have slightly different ability in the solubilization/deaggregation of PDA, which reflects in different concentration of both PDA and its radicals in the solution. In addition to this behaviour,  $[N_{8881}][C_{18:1}]$  appears also to affect the paramagnetic properties of suspended PDA, by favoring the formation of radical species.

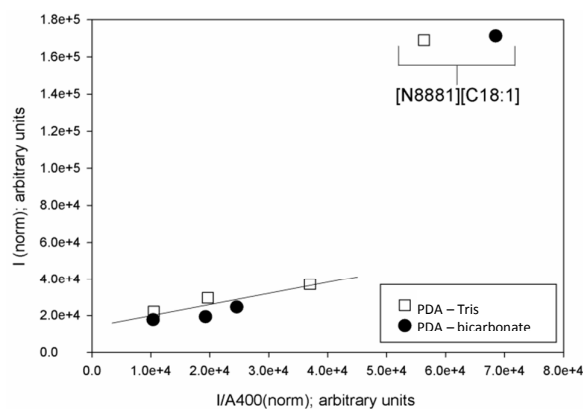
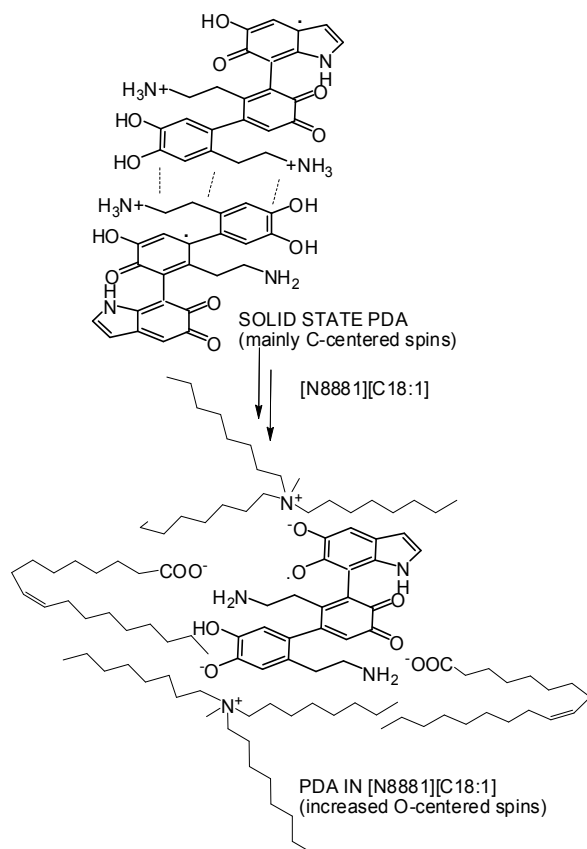


**Figure 5.** Correlation of EPR signal intensity (normalized on linewidth) *versus* the corresponding  $A_{400}$  normalized values for PDA-Tris and PDA-bicarbonate samples.

**A model for PDA paramagnetic behavior based on interaction with ILs.** As per the simplified model previously proposed for synthetic eumelanins,<sup>25</sup> PDA paramagnetism would be due to the

1  
2  
3 contribution of two different free radical populations, *C*-centered ( $g = 2.0032$ ) and *O*-centered ( $g =$   
4  
5 2.0045), the latter of which would predominate as pH increases, due to comproportionation. Based  
6  
7 on this model, it could be argued that for PDA-Tris the passage from the solid state to dispersion in  
8  
9 the ILs is marked by a substantial conversion of the *C*-centered free radicals into *O*-centered  
10  
11 species, a process which is likely assisted by the nitrogenous Tris-derived moieties. A less  
12  
13 pronounced conversion seems to occur in the case of PDA-bicarbonate, for which a similar process  
14  
15 would become more marked in the relatively basic  $[N_{8881}][C_{18:1}]$ . However, signal broadening is the  
16  
17 most relevant spectral change accompanying suspension of PDA-bicarbonate in all ILs, including  
18  
19  $[N_{8881}][C_{18:1}]$ . This behavior of PDA is different from that reported for synthetic 5,6-  
20  
21 dihydroxyindole eumelanins, which did not display line broadening in solution compared to solid  
22  
23 state conditions.<sup>24</sup> It should be noted, however, that in the case of 5,6-dihydroxyindoles the term  
24  
25 “eumelanin solutions” referred to eumelanins *generated* in the presence of polyvinylalcohol, and  
26  
27 not to post-synthetic deaggregation, as in the present case. Several hypotheses can be made to  
28  
29 account for the marked signal broadening in ILs observed herein. A most plausible explanation  
30  
31 would call into play an increase in spin delocalization across the molecular scaffolds consequent to  
32  
33 destacking. Although difficult to verify based on available data, this conclusion would point to the  
34  
35 operation of strong intermolecular interactions in the solid state which appear to “limit” spin  
36  
37 delocalization within aggregated components preventing also extensive conversion of *C*-centered  
38  
39 free radical populations. An alternate view, which would not be exclusive of the former, would  
40  
41 consider line width broadening as the result of specific interactions between the charged  
42  
43 components of ILs and PDA scaffolds, as depicted in Figure 6.  
44  
45  
46  
47  
48  
49  
50  
51  
52  
53  
54  
55  
56  
57  
58  
59  
60



36  
37  
38  
39  
40  
41  
42  
43  
44  
45  
46  
47  
48  
49  
50  
51  
52  
53  
54  
55

**Figure 6.** Schematic illustration of the effect of ILs on PDA spin properties.

56  
57  
58  
59  
60

The detailed nature of free radical species in PDA is unknown, but there is ample evidence that they cannot be effectively represented only by oversimplified schemes based on monomer semiquinones and their equilibria with catechol and quinone species. Wrapping of PDA components within the hydrophobic chains of [N<sub>8881</sub>][C<sub>18:1</sub>] might lead to efficient proton transfer from delocalized semiquinones to carboxylate groups in the IL followed by electrostatic stabilization of the resulting radical anions, showing largely *O*-centered spins. In line with our model, a recent DFT study indicates that *g*-values in the range 2.004-2.005 are not exclusive indicators of neutral semiquinone free radicals as they are also compatible with quinone-like anionic and cationic radicals,<sup>38</sup> which are likely favored in highly polar ionic liquids.

In the proposed scheme, proton transfer to the IL basic groups may occur because of the expectedly high acidity of delocalized semiquinones, exceeding that of the monomers. It is also worth noting

1  
2  
3 that pKa of semiquinones is much lower for catechol units (4.2) than for DHI (7.2), suggesting a  
4  
5 different response of uncyclized versus cyclized structural moieties. In line with this view, the  
6  
7 limited line broadening with dissolution in 1,3-dimethylimidazolium-based ILs may be due to the  
8  
9 lower basicity of the [(CH<sub>3</sub>O)HPO<sub>2</sub>], [(CH<sub>3</sub>O)CH<sub>3</sub>PO<sub>2</sub>] and [(CH<sub>3</sub>O)<sub>2</sub>PO<sub>2</sub>] anionic components.  
10  
11

## 12 13 14 CONCLUSIONS

15  
16 The discovery of the unique ability of ILs to disassemble polymer particles and aggregates to the  
17  
18 nanoscale in a structure-dependent manner may pave the way to novel promising developments in  
19  
20 PDA chemistry and technology. Besides some previous approach based on oxidative treatments,<sup>16,39</sup>  
21  
22 no method has been reported so far, to the best of our knowledge, for the mild non-oxidative and  
23  
24 non-aqueous disassembly and removal of PDA coatings. An important outcome of this study is yet  
25  
26 the first insight and chemical probing of PDA free radical properties made possible by disassembly  
27  
28 to the nanoscale level in ILs. The key finding of the study is the marked alteration of EPR  
29  
30 parameters in an IL structure-dependent manner. A general shift of *g*-factors toward high values  
31  
32 was observed with destacking, which would reflect the effects of removal of the aggregation-  
33  
34 dependent constraints to spin delocalization, as well as the effects of the ionic medium on the  
35  
36 resulting PDA nanostructures. In some instances, a marked line broadening was also apparent in IL,  
37  
38 which would be another consequence of the above effects on spin delocalization. The marked  
39  
40 variations of the EPR response of PDA samples with IL structure revealed specific effects on  
41  
42 exposed electronic spins of potential usefulness for structural investigation. The different EPR  
43  
44 response of PDA samples prepared in Tris and bicarbonate buffers to ILs confirmed moreover the  
45  
46 effect of the medium on PDA structure and properties. An attractive perspective raised by this  
47  
48 study, which is currently under assessment in our laboratories, is the possibility of exploiting a  
49  
50 battery of ILs as chemical probes for comparative EPR scanning of nanoparticles to develop for the  
51  
52 first time a rational picture of IL structure-PDA signal modification relationships as a new approach  
53  
54 to the origin of paramagnetism in melanins. The relevance of this study is related also to the fact  
55  
56  
57  
58  
59  
60

1  
2  
3 that polydopamine films are highly insoluble in most organic solvents and in water unless at  
4  
5 alkaline pHs (>10). The discovery that solvents like ionic liquids are able to disassemble such films  
6  
7 to form a stable suspension of particles is of major importance not only in colloid science but also  
8  
9 for applications in organic synthesis because ionic liquids are more and more considered as ideal  
10  
11 reaction media where polydopamine may play the role of a catalyst for different reactions like  
12  
13 aldolations.<sup>40</sup> The potential technological utility of ILs for de-coating applications warrants further  
14  
15 investigation. The potential technological utility of ILs for de-coating applications is also worthy of  
16  
17 further work.  
18  
19

### 20 21 22 23 **Supporting Information**

24  
25 The Supporting Information is available free of charge via the Internet at <http://pubs.acs.org>.  
26  
27 Experimental details and UV-visible spectra registered on the supernatants obtained from the  
28  
29 treatment of PDA powders with ionic liquids are reported.  
30  
31

### 32 33 34 **ACKNOWLEDGMENT**

35  
36 This work was supported in part by MIUR, PRIN 2010-11 “PROxi” project, and by European  
37  
38 Commission, PolyMed project in the FP7-PEOPLE-2013-IRSES frame (PIRSES-GA-2013-  
39  
40 612538).  
41  
42  
43  
44

### 45 46 **REFERENCES**

- 47  
48 1) Liu, Y.; Ai, K.; Lu, L. Polydopamine and Its Derivative Materials: Synthesis and Promising  
49  
50 Applications in Energy, Environmental, and Biomedical Fields. *Chem. Rev.* **2014**, *114*, 5057–  
51  
52 5115.  
53  
54 2) Kang, S. M.; Hwang, N. S.; Yeom, J.; Park, S. Y.; Messersmith, P. B.; Choi, I. S.; Langer, R.;  
55  
56 Anderson, D. G.; Lee, H. One-Step Multipurpose Surface Functionalization by Adhesive  
57  
58 Catecholamine. *Adv. Funct. Mater.* **2012**, *22*, 2949–2955.  
59  
60

- 1  
2  
3 3) d'Ischia, M.; Napolitano, A.; Ball, V.; Chen, C.-T.; Buehler, M.J. Polydopamine and  
4  
5 Eumelanin: From Structure-Property Relationships to a Unified Tailoring Strategy. *Acc.*  
6  
7 *Chem. Res.* **2014**, *47*, 3541-35.  
8
- 9  
10 4) Nam, H. J.; Kim, B.; Ko, M. J.; Jin, M.; Kim, J. M.; Jung, D. Y. A New Mussel-Inspired  
11  
12 Polydopamine Sensitizer for Dye-Sensitized Solar Cells: Controlled Synthesis and Charge  
13  
14 Transfer. *Chem. Eur. J.* **2012**, *18*, 14000-14007.  
15
- 16  
17 5) Neto, A. I.; Vasconcelos, N. L.; Oliveira, S. M.; Ruiz-Molina, D.; Mano, J. F. High-  
18  
19 Throughput Topographic, Mechanical, and Biological Screening of Multilayer Films  
20  
21 Containing Mussel-Inspired Biopolymers. *Adv. Funct. Mater.* **2016**, *26*, 2745-2755.  
22
- 23  
24 6) Liu, Q.; Wang, N. Y.; Caro, J.; Huang, A. S. Bio-Inspired Polydopamine: A Versatile and  
25  
26 Powerful Platform for Covalent Synthesis of Molecular Sieve Membranes. *J. Am. Chem. Soc.*  
27  
28 **2013**, *135*, 17679–17682.  
29
- 30  
31 7) Pop-Georgievski, O.; Popelka, S.; Houska, M.; Chvostova, D.; Proks, V.; Rypacek, F.  
32  
33 Poly(ethylene oxide) Layers Grafted to Dopamine Melanin Anchoring Layer: Stability and  
34  
35 Resistance to Protein Adsorption. *Biomacromolecules* **2011**, *12*, 3232–3242.  
36
- 37  
38 8) Ju, K.-Y.; Lee, Y.; Lee, S.; Park, S. B. Lee, J.-K. Bioinspired Polymerization of Dopamine to  
39  
40 Generate Melanin-Like Nanoparticles Having an Excellent Free-Radical-Scavenging Property  
41  
42 *Biomacromolecules* **2011**, *12*, 625-632.  
43
- 44  
45 9) Rodriguez, C.; Rebeca, A.; Saiz-Poseu, J.; Garcia-Pardo, J.; Garcia, B.; Lorenzo, J.; Ojea-  
46  
47 Jimenez, I.; Komilis, D.; Sedo, J.; Busque, F. et al. *RSC Advances* **2016**, *6*, 40058-40066.  
48
- 49  
50 10) Quignard, S.; Chen, Y.; d'Ischia M.; Fattaccioli, J. UV-Induced Fluorescence of  
51  
52 Polydopamine-Coated Emulsion Droplets. *ChemPlusChem* **2014**, *79*, 1254-1257.  
53
- 54  
55 11) Kang, K.; Choi, I. S.; Nam, Y. A Biofunctionalization Scheme for Neural Interfaces Using  
56  
57 Polydopamine Polymer. *Biomaterials* **2011**, *32*, 6374–6380.  
58  
59  
60

- 1  
2  
3 12) Yildirim, A.; Bayindir, M. Turn-on Fluorescent Dopamine Sensing Based on in Situ  
4 Formation of Visible Light Emitting Polydopamine Nanoparticles. *Anal. Chem.* **2014**, *86*,  
5 5508–5512.  
6  
7  
8  
9  
10 13) Lin, J.-H.; Yu, C.-J.; Yanga, Y.-C.; Tseng, W.-L. Formation of Fluorescent Polydopamine  
11 Dots from Hydroxyl Radical-Induced Degradation of Polydopamine Nanoparticles.  
12 *Phys. Chem. Chem. Phys.*, **2015**, *17*, 15124-151-30.  
13  
14  
15  
16 14) Zheng, L.; Xiong, L.; Zheng, D.; Li, Y.; Liu, Q.; Han, K.; Liu, W.; Tao, K.; Yang, S.; Xia, J.  
17 Bilayer Lipid Membrane Biosensor with Enhanced Stability for Amperometric Determination  
18 of Hydrogen Peroxide. *Talanta*, **2011**, *85*, 43–48.  
19  
20  
21  
22  
23 15) Cui, J.; Yan, Y.; Such, G.K.; Liang, K.; Ochs, C.J.; Postma, A.; Caruso, F. Immobilization  
24 and Intracellular Delivery of an Anticancer Drug Using Mussel-Inspired Polydopamine  
25 Capsules. *Biomacromolecules* **2012**, *13*, 2225-2228.  
26  
27  
28  
29  
30 16) Chen, X.; Yan, Y.; Müllner, M.; van Koeveden, M.P.; Noi, K.F.; Zhu, W.; Caruso, F.  
31 Engineering Fluorescent Poly(dopamine) Capsules. *Langmuir* **2014**, *30*, 2921-2925.  
32  
33  
34 17) Della Vecchia, N. F.; Avolio, R.; Alfè, M.; Errico, M. E.; Napolitano, A.; d'Ischia, M.  
35 Building-Block Diversity in Polydopamine Underpins a Multifunctional Eumelanin-Type  
36 Platform Tunable Through a Quinone Control Point. *Adv. Funct. Mater.* **2013**, *23*, 1331-1340.  
37  
38  
39  
40 18) Liebscher, J.; Mrowczynski, R.; Scheidt, H. A.; Filip, C.; Hadade N. D.; Turcu, R.; Bende, A.;  
41 Beck S. Structure of Polydopamine: A Never-Ending Story? *Langmuir* **2013**, *29*,  
42 10539–10548.  
43  
44  
45  
46  
47 19) Dreyer, D. R.; Miller, D. J.; Freeman, B. D.; Paul, D. R.; Bielawski, C. W. Perspectives on  
48 Poly(dopamine). *Chem. Sci.* **2013**, *4*, 3796–3802.  
49  
50  
51  
52 20) Della Vecchia, N.F.; Luchini, A.; Napolitano, A.; D'Errico, G.; Vitiello, G.; Szekely, N.;  
53 d'Ischia, M.; Paduano, L. Tris Buffer Modulates Polydopamine Growth, Aggregation, and  
54 Paramagnetic Properties. *Langmuir* **2014**, *30*, 9811-9818.  
55  
56  
57  
58  
59  
60

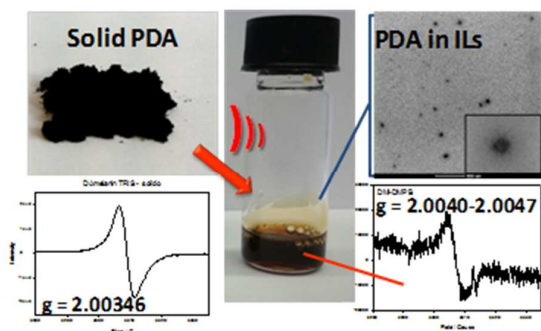
- 1  
2  
3 21) Ponzio, F.; Barthès, J.; Bour, J.; Michel, M.; Bertani, P.; Hemmerlé, J.; d'Ischia, M.; Ball, V.  
4  
5 Oxidant Control of Polydopamine Surface Chemistry in Acids: A Mechanism-Based Entry to  
6  
7 Superhydrophilic-Superoleophobic Coatings. *Chem. Mater.* **2016**, *28*, 4697–4705.  
8  
9  
10 22) Yang, Y.; Qi, P.; Ding, Y.; Maitz, M.F.; Yang, Z.; Tu, Q.; Xiong, K.; Leng, Y.; Huang, N. A  
11  
12 Biocompatible and Functional Adhesive Amine-Rich Coating Based on Dopamine  
13  
14 Polymerization. *J. Mater. Chem. B*, **2015**, *3*, 72–81.  
15  
16  
17 23) Ambrico, M.; Ambrico, P.F.; Cardone, A.; Della Vecchia, N.F.; Ligonzo, T.; Cicco, S.R.;  
18  
19 Talamo, M.M.; Napolitano, A.; Augelli, A.; Farinola, G.M. et al. Engineering Polydopamine  
20  
21 Films with Tailored Behaviour for Next-Generation Eumelanin-Related Hybrid Devices. *J.*  
22  
23 *Mat. Chem C*, **2013**, *1*, 1018-1028.  
24  
25  
26 24) Panzella, L.; Gentile, G.; D'Errico, G.; Della Vecchia, N.F.; Errico, M.E.; Napolitano, A.;  
27  
28 Carfagna, C.; d'Ischia, M. Atypical Structural and  $\pi$ -Electron Features of a Melanin Polymer  
29  
30 That Lead to Superior Free-Radical-Scavenging Properties. *Angew. Chem. Int. Ed.* **2013**,  
31  
32 *52*, 12684-12687.  
33  
34  
35 25) Mostert, A. B.; Hanson, G. R.; Sarna, T.; Gentle, I. R.; Powell, B. J.; Meredith, P. Hydration-  
36  
37 Controlled X-Band EPR Spectroscopy: A Tool for Unravelling the Complexities of the Solid-  
38  
39 State Free Radical in Eumelanin. *J. Phys. Chem. B* **2013**, *117*, 4965–4972.  
40  
41  
42 26) Mrówczyński, R.; Emerson Coy, L.; Scheibe, B.; Czechowski, T.; Augustyniak-Jabłokow,  
43  
44 M.; Jurga, S.; Tadyszak, K. Electron Paramagnetic Resonance Imaging and Spectroscopy of  
45  
46 Polydopamine Radicals *J. Phys. Chem. B* **2015**, *119*, 10341–10347.  
47  
48  
49 27) Vogel, R.; Dobe, C.; Whittaker, A.; Edwards, G.; Riches, J. D.; Harvey, M.; Trau,  
50  
51 M.; Meredith, P. Postsynthesis Stabilization of Free-Standing Mesoporous Silica Films.  
52  
53 *Langmuir* **2004**, *20*, 2908-2914.  
54  
55  
56 28) Wakasa, M. The Magnetic Field Effects on Photochemical Reactions in Ionic Liquids *J. Phys.*  
57  
58 *Chem. B* **2007**, *111*, 9434– 9436.  
59  
60

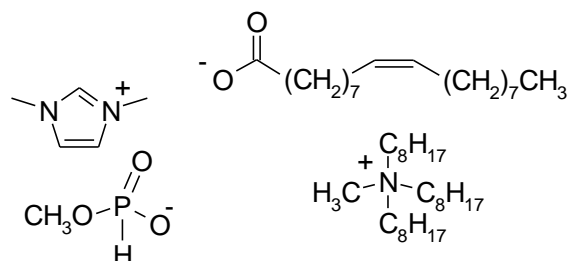
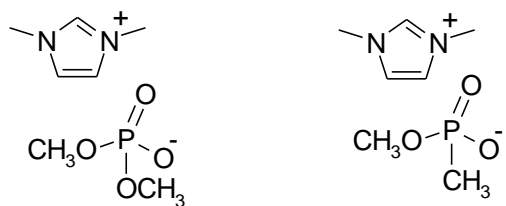
- 1  
2  
3 29) Takahashi, K.; Tezuka, H.; Kitamura, S.; Satoh, T.; Katoh, R. Reactions of Excited-State  
4 Benzophenone Ketyl Radical in a Room-Temperature Ionic Liquid. *Phys.Chem.Chem.Phys.*  
5 **2010**, *12*, 1963–1970.  
6  
7  
8  
9  
10 30) Yang, Y; Fan, H.; Song, J; Meng, Q.; Zhou, H.; Wu, L.; Yang, G; Han, B. Free Radical  
11 Reaction Promoted by Ionic Liquid: a Route for Metal-Free Oxidation Depolymerization of  
12 Lignin Model Compound and Lignin. *Chem. Commun.* **2015**, *51*, 4028-4031.  
13  
14  
15  
16 31) Parmentier, D.; Metz, S.J.; Kroon, M.C. Homogeneous Liquid-Liquid Extraction of Rare  
17 Earths with the Betaine-Betainium Bis(trifluoromethylsulfonyl)imide Ionic Liquid System.  
18 *Green Chem.*, **2013**, *15*, 205-209.  
19  
20  
21  
22  
23 32) Ponzio, F.; Barthes, J.; Bour, J.; Michel, M.; Bertani, P.; Hemmerlé, J.; d'Ischia, M.; Ball, V.  
24 Oxidant Control of Polydopamine Surface Chemistry in Acids: A Mechanism-Based Entry to  
25 Superhydrophilic-Superoleophobic Coatings. *Chem. Mater.* **2016**, *28*, 4697–4705  
26  
27  
28  
29 33) Palgunadi, J.; Yun Hong, S.; Kyu Lee, J.; Lee, H.; Deuk Lee, S.; Cheong, M., Sik Kim, H.  
30 Correlation between Hydrogen Bond Basicity and Acetylene Solubility in Room Temperature  
31 Ionic Liquids. *J. Phys. Chem. B* **2011**, *115*, 1067–1074.  
32  
33  
34  
35  
36 34) Hayes, R.; Warr, G.G.; Atkin, R. Structure and Nanostructure in Ionic Liquids. *Chem. Rev.*  
37 **2015**, *115*, 6357–6426.  
38  
39  
40  
41 35) Acik, M.; Dreyer, D.R.; Bielawski, C.W.; Chabal, Y.J. Impact of Ionic Liquids on the  
42 Exfoliation of Graphite Oxide *J. Phys. Chem. C* **2012**, *116*, 7867–7873.  
43  
44  
45 36) Pilawa, B.; Buszman, E.; Wrześniok, D.; Latocha, M.; Wilczok, T. Application of EPR  
46 Spectroscopy to Examination of Gentamicin and Kanamycin Binding to DOPA-Melanin.  
47 *Appl. Magn. Reson.* **2002**, *23*, 181–192.  
48  
49  
50  
51 37) Meredith, P.; Sarna, T. *Pigment Cell Res.* **2006**, *19*, 572-594.  
52  
53  
54 38) Batagin-Neto, A.; Soares Bronze-Uhle, E.; de Oliveira Graeff, C.F. Electronic Structure  
55 Calculations of ESR Parameters of Melanin Units. *Phys. Chem. Chem. Phys.* **2015**, *17*, 7264-  
56 7274.  
57  
58  
59  
60

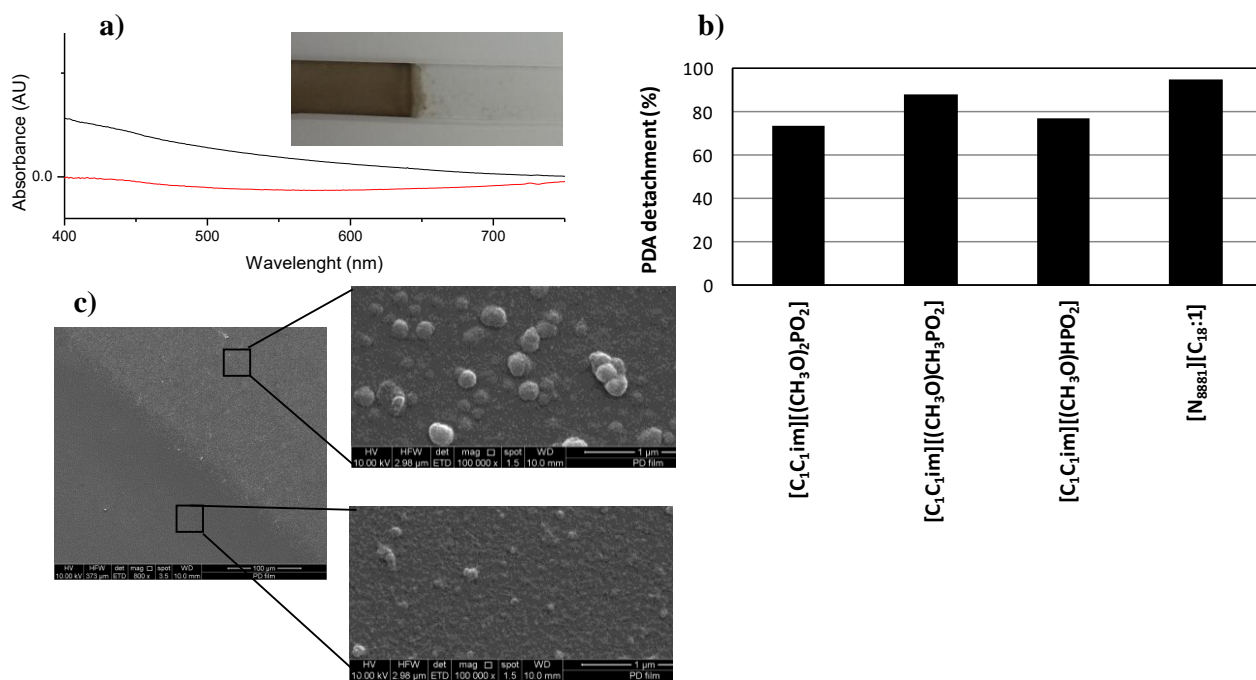
- 1  
2  
3 39) Ball, V.; Del Frari, D.; Toniazzo, V.; Ruch, D. Kinetics of Polydopamine Film Deposition as  
4 a Function of pH and Dopamine Concentration: Insights in the Polydopamine Deposition  
5 Mechanism. *J. Colloid Interf. Sci.* **2012**, *386*, 366-372.  
6  
7  
8  
9 40) Mrówczyński, R.; Bunge, A.; Liebscher, J. Polydopamine-an Organocatalyst Rather Than an  
10 Innocent Polymer. *Chem. Eur. J.* **2014**, *20*, 8647-8653.  
11  
12  
13  
14  
15  
16  
17  
18  
19  
20  
21  
22  
23  
24  
25  
26  
27  
28  
29  
30  
31  
32  
33  
34  
35  
36  
37  
38  
39  
40  
41  
42  
43  
44  
45  
46  
47  
48  
49  
50  
51  
52  
53  
54  
55  
56  
57  
58  
59  
60

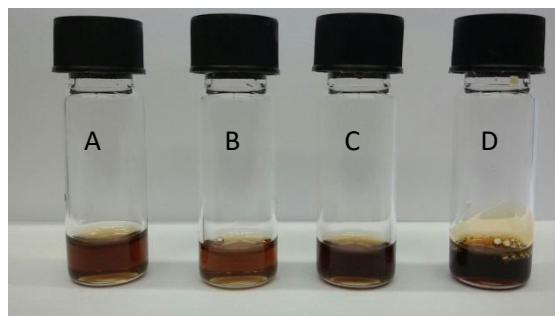
## Table of Contents

**Ionic Radical:** Sonication of polydopamine (PDA) in different ionic liquids (ILs) resulted in the generation of nanostructures with marked alterations of the electron paramagnetic resonance properties, suggesting destacking-related free radical reorganization driven by ionic interactions.









1  
2  
3  
4  
5  
6  
7  
8  
9  
10  
11  
12  
13  
14  
15  
16  
17  
18  
19  
20  
21  
22  
23  
24  
25  
26  
27  
28  
29  
30  
31  
32  
33  
34  
35  
36  
37  
38  
39  
40  
41  
42  
43  
44  
45  
46  
47  
48  
49  
50  
51  
52  
53  
54  
55  
56  
57  
58  
59  
60

1  
2  
3  
4  
5  
6  
7  
8  
9  
10  
11  
12  
13  
14  
15  
16  
17  
18  
19  
20  
21  
22  
23  
24  
25  
26  
27  
28  
29  
30  
31  
32  
33  
34  
35  
36  
37  
38  
39  
40  
41  
42  
43  
44  
45  
46  
47  
48  
49  
50  
51  
52  
53  
54  
55  
56  
57  
58  
59  
60

